

Processing and levitation force in top-seeded YBCO

R. Yu, J. Mora, S. Piñol, F. Sandiumenge, N. Vilalta, V. Gomis, B. Martínez, E. Rodríguez, J. Amoros, M. Carrera, X. Granados, D. Camacho, J. Fontcuberta, and X. Obradors

Institut de Ciència de Materials de Barcelona, CSIC, 08193 Bellaterra, Spain

Abstract--Bulk cylinders of $\text{YBa}_2\text{Cu}_3\text{O}_7\text{-Y}_2\text{BaCuO}_5$ composites, up to 35.0 mm in diameter, have been melt-processed using MgO single crystals, Nd123 and Sm123 melt textured ceramics, as seeds. The influence of processing parameters has been examined in order to optimize the growth conditions. Polarized light microscopy, SEM and ^3DX , have been used to characterize the orientation, size and morphology of the grains, as well as the spatial distribution and size of Y211 particles. An increase of the levitation forces is observed when the top seeding growth is carried out under a temperature gradient. The trapped magnetic and the levitation force of a single domain sample was systematically measured and theoretically simulated by finite element calculations. The deduced J_c from the different experiments have been compared and analyzed.

I. INTRODUCTION

High levitation forces in Y123 can be achieved by optimizing the flux pinning and increasing the size of well-oriented grains. The strength of the flux pinning can be enhanced by suitable additions such as CeO_2 [1] and microstructural defects [2] into the materials. The orientation of the domains with respect to the upper surface of the cylinder can be controlled by seeding and solidification in a temperature gradient [3][4]. The maximum levitation force is achieved when the a-b planes are perpendicular to the applied field. Currently, different seeds, such as MgO single crystals, Nd123 and Sm123 melt textured materials, have been used to fabricate bulk Y123 cylinders.

In this paper we report our recent work on the directional solidification of Y123 bulk cylinders from the partial melt using MgO, Nd123 and Sm123 seeds. The samples were fabricated either with a temperature gradient or isothermally. The influence of the processing parameters on the microstructure and the levitation force will be discussed.

II. EXPERIMENTAL

Large cylindrical bulk samples ($\varnothing=35.0$ mm, height $t=25.0$ mm) with initial composition Y123 + 15.0 % Y211 + 1.0 % CeO_2 were fabricated by slow cooling through the peritectic temperature. The cylinders were grown, either in a six-faces heated isothermal furnace, or in a furnace with a temperature gradient ($G \approx 10$ °C/cm). The effectiveness of different seeds, MgO, Nd123 and Sm123, was investigated. Single domain Nd123 and Sm123 samples with high T_c were prepared using a Bridgman method[5].

The microstructure has been analyzed using polarized light and scanning electron microscopy. Superconducting

properties were characterized by levitation force, inductive critical current measurements with a SQUID magnetometer and mapping of the remanent magnetic flux as measured by Hall microprobes (active surface of $100 \times 100 \mu\text{m}^2$).

III. RESULTS AND DISCUSSIONS

A. Seed and Substrate Materials

In melt-texturing of YBCO samples, it is essential to avoid the loss of liquid phase, because it may cause a significant change of the Y211 concentration and a perturbation of the growth process. In our study, two methods were used to reduce the liquid loss: (1) Addition of secondary phases like Y211 and CeO_2 , which increase the capillarity of the partial melt; and (2) sintered CeO_2 ceramics was selected as substrate with a minimum contact area with the sample. It was found that the liquid losses were significantly reduced by adopting both methods. Energy dispersive X-ray (EDX) mapping of Y, Ba, Cu, and Ce indicated a uniform composition through the samples.

To reach a complete understanding of the main factors controlling the solidification process we performed a multivariable analysis (see Table I). We first carried out a series of tests (group A) where the maximum heating temperature was changed while G and V (cooling rate) were fixed. In the B group we only modified the cooling rate, V , and in group C two types of seeds were used with or without temperature gradient. Here we will focus on the results obtained with MgO and Nd123 seeds. The size of the seeds was about 16 mm^2 . They were always placed on the center of the upper surface of the cylindrical pellet after careful polishing.

B. Microstructure

For the samples processed in isothermal conditions and without seed, the typical grain size was 4-5 mm. As the sample was cooled down through the peritectic temperature, YBCO crystals nucleated simultaneously at the top and lateral surfaces of the sample, and the growth proceeded along

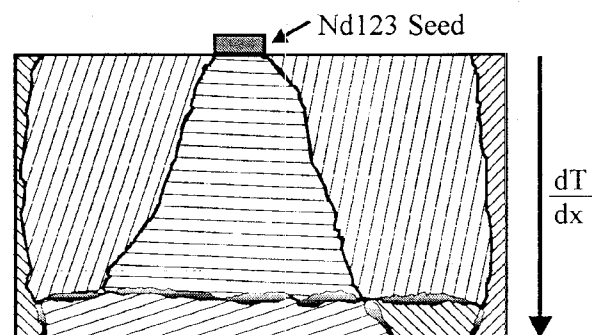


Fig.1. Schematic representation of the grains in YBCO cylinders with MgO and Nd123 seeds.

Manuscript received August 26, 1996.

This work was supported by MIDAS program (92-2331), CICYT (MAT91-0742) and EC (BRE2-CT94-1011).

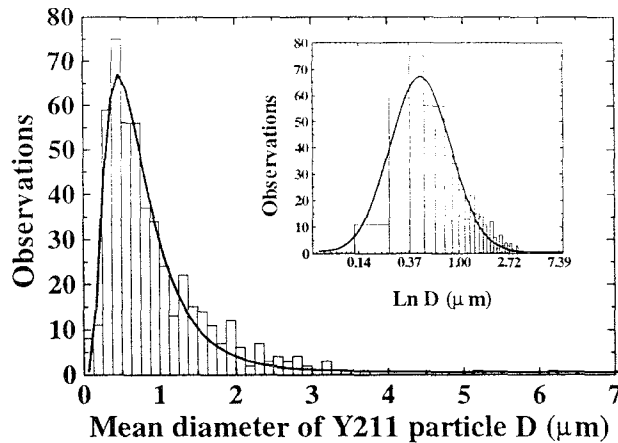


Fig.2. Histogram of Y211 particle size in YBCO cylinders prepared using a Nd123 seed and with a temperature gradient. The solid line is the fitting to a log-normal distribution. The inset shows the same result in a logarithmic scale and the fitting to a Gaussian distribution.

different directions. In this case some Y211 phase was accumulated in the center of the sample. When a seed crystal was placed on the top of the sample, still in isothermal conditions, large grains (~15.0 mm) of YBCO were achieved with the orientation determined by the seed, i.e. the a-b planes parallel to the upper surface of the cylinder. In this case, SEM-EDX microstructural analysis revealed that large grains were indeed nucleated at the seed. However, the seeded growth front was interrupted at about the center of the sample as a result of its impingement with other grains nucleated at different points of the surface.

In order to avoid nucleation of the grains from the bottom and lateral surface of the sample, the growth was performed with a temperature gradient of 10 °C/cm. In this case, the nucleation was restricted to the top surface and the growth proceeded down to the bottom of the sample. However, some accumulation of excess Y211 phase and porosities was often found in the lower part near the bottom of the sample (see Fig. 1). This phenomenon may be related to the loss of liquid and incomplete peritectic reaction because the cooling rate was probably too high (2 °C/h). Seeding with different crystals, in combination with the temperature gradient, resulted in a large grain (~20.0 mm) growing along the c-axis, i.e. growing epitaxially from the seed crystals.

Although the liquid loss was significantly reduced by the addition of Y211 and CeO₂ together with the adoption of CeO₂ substrate, it was not completely eliminated. EDX experiments indicated that the CeO₂ substrate reacted with the melt forming some phases rich in Ba and Cu, which resulted in a depletion of these elements in YBCO matrix near the substrate. The loss of liquid phase due to the reaction between the substrate and melt could be another reason for the accumulation of Y211 phase in the sample.

The size and the concentration of the porosities and Y211 phase could be reduced by decreasing the cooling rate through the peritectic temperature. For the sample processed

TABLE I
PROCESSING PARAMETERS AND LEVITATION FORCES

Exp.	T ^{max} (°C)	Seed	V(°C/h)	G(°C/cm)	F ^{max} (N)	F ^{max} /F ^{Meiss} (%)
A	1060	-	2	10	14	19.7
	1080	-	2	10	20	28.1
	1120	-	2	10	21	29.3
B	1060	-	1	10	15	21.1
	1060	MgO	2	-	18	25.3
C	1060	Nd123	2	-	21	29.3
	1060	MgO	2	10	20	28.1
	1060	Nd123	2	10	25	35.2

at V=1.0 mm/h, no accumulation of Y211 phase occurred at the bottom of the pellet.

When the growth was carried out in a temperature gradient but without seeding, the orientation of the domains was found to depend in a reproducible way on the holding temperature T_{max}. For T_{max}=1060 °C, the a-b planes are preferentially aligned at a small angle of the sample axis, i.e. the direction of temperature gradient. As the holding temperature was increased, the angle between the a-b planes and the sample axis was increased too. For T_{max}=1120 °C, the a-b planes of the central large grains are nearly perpendicular to the sample axis, even if the sample was processed at V=2.0 °C/h. The exact origin of this phenomenon is not clear at the moment, but it has already been observed by other authors [6].

Y211 particles size and their distribution were determined from SEM pictures analysis of fractured surfaces using an automated image analysis system. Fig. 2 shows the typical size distribution of entrapped Y211 particles in the Nd123 top seeded sample prepared with temperature gradient at V=2.0 °C/h. The results are very similar to those observed for the Bridgman grown samples where a homogeneous size distribution is observed [7]. Fitting the experimental data to a log-normal distribution equation (see solid line in Fig. 2), the

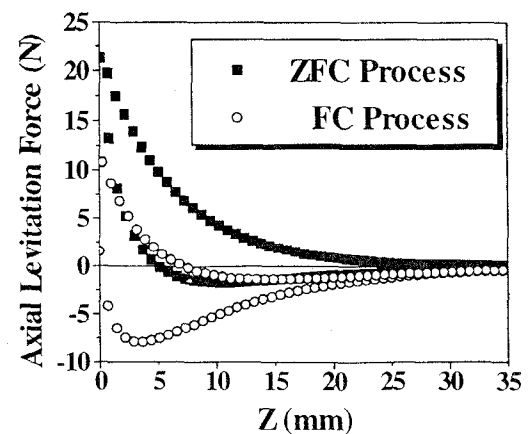


Fig. 3. Axial Levitation Force at the Zero Field Cooled Process (solid symbol) and Field Cooled Process (open symbol).

average particle diameter ($\bar{D}=0.46 \mu\text{m}$) and standard deviation factor ($\sigma=0.60$) were obtained.

C. Levitation force measurements

The levitation forces were measured with a SmCo magnet ($\varnothing=30.0 \text{ mm}$, $t=20.0 \text{ mm}$) with $B_r \approx 0.3 \text{ T}$ moving at 0.1 mm/s relative to the SC. A typical levitation force measurement at ZFC and FC condition are indicated in Fig. 3 while the maximum levitation force in ZFC, $F^{\text{max}}(\text{N})$, for different samples, are indicated in Table I. These results can be summarized as follows:

1. The top-seeded samples, having a higher surface with the a-b planes perpendicular to the sample axis, exhibit larger levitation force compared with the samples prepared without seeding.

2. The levitation force increases with the holding temperature for samples prepared with temperature gradient without seeding.

Both results indicate that the levitation force is critically dependent on the orientation of the grains due to the anisotropic behavior of YBCO crystals. The maximum levitation force was found for the samples grown with Nd123 seeds in a temperature gradient.

In order to normalize the levitation force measurements we have theoretically calculated the maximum levitation force corresponding to the Meissner state[8] for the superconductor sample (see Table I). The levitation force in the Zero Field Cooled (ZFC) process, measured using our experimental setup, reaches up to 35 % of the theoretical limit which is similar to that reported recently [9]. It is important to stress that for a first approximation this ratio is independent of the strength of the permanent magnet and therefore can be used to assess the quality of the samples. It should be mentioned, however, that the measured levitation force is slightly dependent on the moving velocity of the magnet (0.1 mm/s in the present experiments) because of flux creep effects [10].

D. Critical Currents and levitation force modeling

As we have previously described the levitation forces in the large diameter samples are mainly determined by the size and the orientation of the domains. Therefore, in order to

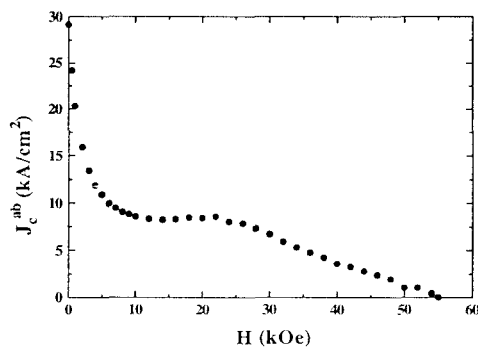


Fig. 4. Critical current (H/c , $T=77 \text{ K}$) as a function of the applied magnetic field for YBCO pellets processed at cooling rate of 1°C/h .

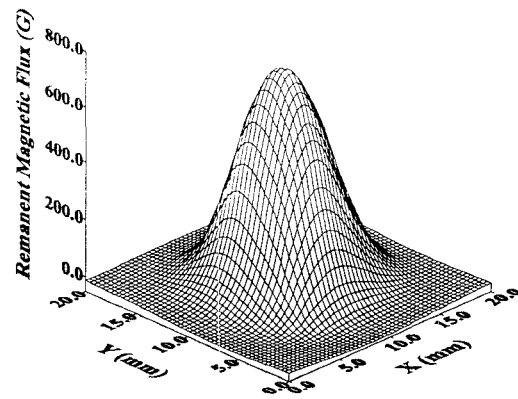


Fig.5. Magnetic flux profile after a Field Cooled process for the single domain sample.

analyze in detail the superconducting behavior of the large single domains and to test the self-consistency of the experimental methodologies being used to characterize the samples, we have isolated a single domain sample and we have measured its inductive critical current with the SQUID magnetometer, the levitation force and the remanent magnetic flux profile.

From a sample grown by the B process (see Table I) a single domain has been cut with a rectangular shape of dimensions $10.0 \times 9.0 \times 4.0 \text{ mm}^3$. A single domain sample with a cubic dimension of about 1 mm^3 has been also cut from the same cylinder for the SQUID measurements. The critical current deduced from the hysteresis loop measured at 77 K is represented in Fig. 4 where it is clearly appreciated that the observed J_c values are not yet fully optimized as in Bridgman grown samples where values as high as 10^5 A/cm^2 are observed [11]. Remanent magnetic flux measurements were performed in order to test the superconducting behavior of the whole single domain. A Hall microprobe was scanned at 0.5 mm from the surface after cooling in the field generated by the same SmCo magnet used in the levitation force measurements. The results are reported in Fig. 5 where a single peak is observed thus allowing us to ascertain that the sample has, indeed, a single domain character. Finally, the dependence of the maximum trapped field on the external magnetic field was investigated up to 2 T and a saturation was found at $B^{\text{rem}} \sim 980 \text{ G}$ which indicate that $H^* \sim 1600 \text{ Oe}$.

From the mapping of the remanent magnetic flux, the critical current was deduced by solving the inverse problem to determine the current density distribution [12]. Minor asymmetries of the current distribution may be observed in Figure 6 which are originated by the slightly non-symmetrical behavior of the experimental $B_z(x,y)$ values and which indicate that the single domain samples grown by the top seeding technique may bear some microstructural inhomogeneities. The calculated current distribution is consistent with a penetration state such that $H^{\text{max}} \sim 2H^*$ in agreement with the high field remanence measurements. The calculated J_c values, either from the current distribution (Fig. 6) and from the saturated magnetic remanence are in the

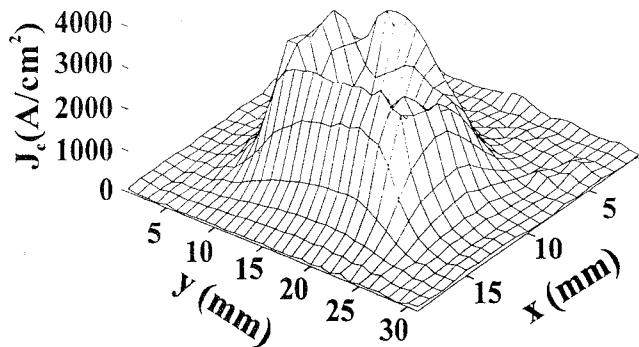


Fig. 6. Calculated current density distribution in a single domain sample.

range $3.5 \times 10^3 - 4.0 \times 10^3$ A/cm². Both calculations lead to consistent J_c values which are somewhat smaller than those deduced from inductive measurements in smaller samples (Fig. 4) thus suggesting that there is a length scale effect, probably related to the inhomogeneous microstructure [13], in the irreversible magnetic properties of the top-seeded melt textured YBCO superconductors.

Finally, levitation forces simulation was performed with a finite element analysis software to analyze further the consistency of the irreversible superconducting properties and to define a tool for the evaluation of the quality of the samples as it has been recently suggested [9] (see Table I). Two kind of superconductor states have been simulated: the Meissner state and the flux penetration under zero field cooled conditions assuming a critical state with the Bean approximation. In both cases a cylindrical geometry was used.

For the simulation in the Meissner state, a zero flux density has been imposed inside the superconductor setting a null magnetic potential vector ($\vec{A}=0$) or a null magnetic permeability ($\mu=0$) as boundary condition. The percentage between this limit and the maximum measured force in the single domain sample is about 50 % (Fig. 7) which could be even slightly increased with a closer diameter between the permanent magnet and the superconductor [8]. We note that this force percentage is considerably higher than those observed in multidomain samples (Table I). This allows us to estimate that a single domain cylinder with the geometrical dimensions used in the present work and with the corresponding permanent magnet would present $F^{\max}=35.5$ N.

The simulation of the levitation force when a critical state is established was modeled using an hysteretic BH curve assuming the Bean model (Fig. 7). The fit of the calculated levitation forces to the experimental values leads to $J_c=1.5 \times 10^4$ A/cm², in very good agreement with the inductive measurements and hence somehow higher than the evaluation performed from the magnetic remanence measurements. The origin of this discrepancy is not completely clear at present but it is very likely that the geometrical effects have a different weight in the different experiments.

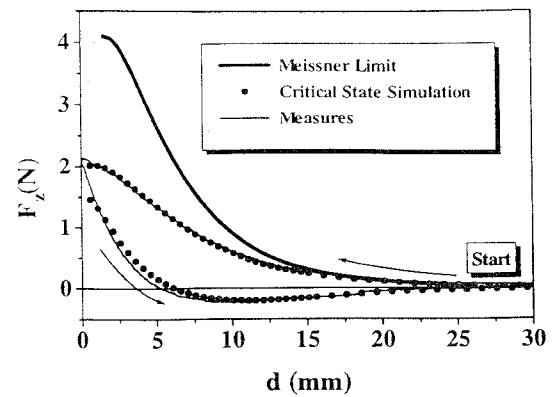


Fig. 7. Representation of the measured levitation force for a single domain sample (thin solid line) and the results of finite element simulations (solid dots). The thick solid line is the theoretical maximum force.

IV. CONCLUSIONS

We have demonstrated that directional solidification of bulk Y123 cylinders by combining seeding and temperature gradient, allows the fabrication of samples having an optimum orientation and large grains, rendering to larger levitation forces. However undesired crystal nucleation still occurs and thus further refinement of the processing conditions appears necessary. In particular we have observed that increasing the holding temperature above T_p leads to an enhanced levitation force. The relationship between critical currents, magnetic remanence and levitation force has been experimentally and theoretically analyzed using a finite element simulation and solving the inverse problem.

REFERENCES

- [1] S. Piñol, F. Sandiumenge, B. Martínez, V. Gomis, J. Fontcuberta, X. Obradors, E. Snoeck, and Ch. Roucau, *Appl. Phys. Lett.*, vol. 65, pp. 1448, 1994.
- [2] M. Murakami, *Melt Textured Processed High-Temperature Superconductors*, World Scientific, Singapore, 1992.
- [3] L. Gao, Y. Y. Xue, D. Ramirez, Z. L. Huang, R. L. Meng, and C. W. Chu, *Appl. Phys. Lett.*, vol. 63, pp. 260, 1993.
- [4] D. F. Lee, C. S. Partinevelos, R. G. Presswood, Jr, and K. Salama, *J. Appl. Phys.*, vol. 76, pp. 603, 1994.
- [5] S. Piñol, V. Gomis, B. Martínez, A. Labarta, and X. Obradors, *J. Alloys and Compounds*, vol. 195, pp. 11, 1993.
- [6] A. M. M. Barus, and J. A. T. Taylor, *Physica C*, vol. 258, pp. 308, 1996.
- [7] N. Vilalta, F. Sandiumenge, S. Piñol, and X. Obradors, *J. Mater. Res.*, in press.
- [8] D. Camacho et al. to be published.
- [9] T. Straßer, T. Habisreuther, W. Gawalek, M. Wu, D. Litzkendorf, P. Gömert, K. V. Iljushin and L. J. Kovaljov, in *Applied Superconductivity 1995*, Inst. Phys. Conf. Ser. No148, Ed.D.Dew-Huges (Inst. of Physics Publ.), vol 1, pp. 687, 1995.
- [10] P. Boegler, C. Urban, H. Rietschel and H. J. Bornemann, *Appl. Superconductivity*, vol. 2, No. 5, pp. 315-325, 1994.
- [11] B. Martínez, X. Obradors, A. Gou, V. Gomis, S. Piñol, J. Fontcuberta, H. van Tol, *Phys. Rev. B*, vol. 53, pp. 2797, 1996.
- [12] W. Xing, B. Heinrich, Hu Zhou, A. A. Fife and A. R. Cragg, *J. Appl. Phys.*, vol. 76, pp. 4244, 1994.
- [13] F. Sandiumenge, N. Vilalta, X. Obradors and S. Piñol, *J. Appl. Phys.*, vol. 79, pp. 8847, 1996.